

# Prediction of grinding parameters for plastics by artificial neural networks

David Samek, Ondrej Bilek, and Jakub Cerny

**Abstract**— The grinding technology is widely used in the manufacturing of various materials. This technology process is driven by many input parameters that influence resulting product. This work is focused on an application of artificial neural network with radial basis function in modeling of polymer materials grinding. In this paper the two key parameters were selected – feed rate and depth of cut. The task of the artificial neural network based predictor is to provide resulting arithmetical mean roughness and maximum height of the profile parameter. Furthermore, the article presents extensive experimental measurements aimed to grinding of polypropylene, polyamide 6 filled with 30% of glass fibers, polytetrafluoro-ethylene and polycarbonate. All measurements results are statistically evaluated and presented in the figures.

**Keywords**— artificial neural networks, grinding, prediction, radial basis function.

## I. INTRODUCTION

**G**RINDING is the finishing machining operation to ensure the final surface quality. Compared with the operation methods of defined tool geometry, a tool for grinding consists of a number of statistically oriented grinding grains of random shapes. During the grinding process, small chips are removed along with high rates of material removal. Therefore grinding operations are used for machining difficult-to and hardened materials. Grinding polymers, and in the case of this article predominantly thermoplastics [7], it is difficult due to their nature [16]. Despite this fact, grinding is widely used in the plastics industry for the clean-up of intake gates and overflows. Grinding is recommended as a secondary processing for prototyping and low complex parts made from blanks and it is suitable to making thick or tight tolerance parts. Grinding thermoplastics is difficult because of their relatively low melting temperature and plasticity point,

Manuscript received June 27, 2011. Revised version received June 30, 2011. This article is financially supported by the Ministry of Education, Youth and Sports of the Czech Republic under the Research Plan No. MSM 7088352102 and by the European Regional Development Fund under the project CEBIA-Tech No. CZ.1.05/2.1.00/03.0089.

D. Samek is with the Department of Production Engineering, Faculty of technology, Tomas Bata University in Zlin, nam. T. G. Masaryka 5555, 76001 Zlin, Czech Republic (phone: +420-576-035-157; fax: +420-576-035-176; e-mail: samek@ft.utb.cz).

O. Bilek is with the Department of Production Engineering, Faculty of technology, Tomas Bata University in Zlin, nam. T. G. Masaryka 5555, 76001 Zlin, Czech Republic (e-mail: bilek@ft.utb.cz).

J. Cerny is with the Department of Production Engineering, Faculty of technology, Tomas Bata University in Zlin, nam. T. G. Masaryka 5555, 76001 Zlin, Czech Republic (e-mail: jlcerny@ft.utb.cz).

resulting in the clogging of surface grinding wheel. It is recommended to use a grinding wheel with more open spaces between the grains, together with the excessive amount of coolant to prevent overheating and clogging of the grinding wheel [19], [20].

The resulting surface quality depends on input factors such as principally cutting conditions are, followed by grinding material and accompanying phenomena [8], [9]. Generally, materials hard to machine are ground by finer grit wheels and a soft materials are ground by coarse grained wheels. Cutting speed strongly influences the selection of a suitable grinding wheel degree. It is known that the higher cutting speed is, the finer the grinding wheel should be. The choice of optimal cutting conditions for grinding is not as strongly influenced by the requirement of keeping the optimum tool life, as is the case with other machining methods.

Since grinding is mostly used as finishing method, which determines the functional properties of the surface, the knowledge of the surface quality and its control are crucial. It is therefore an effort to achieve high levels of surface quality; conditionally improved by the grinding process, choosing the appropriate cutting conditions. The quality of grinded surface is generally defined as the sum of the properties under consideration upon demands. It is a complex of system factors. Surface quality includes physical, chemical and geometric properties [10]. The geometric surface properties include roughness parameters as a characteristic of micro geometry in the cut plane perpendicular to the surface [18].

Artificial neural networks (ANNs) are commonly used for modeling of technological processes [1]-[6]. Typically multilayered feed-forward neural networks [12]-[15] are utilized. However, these ANNs do not provide sufficient results in all applications [17]. Therefore, it should be considered other types of artificial neural networks such as recurrent neural networks or neural networks with radial basis function (RBF). This paper focuses on application of the radial basis function neural networks, because they offer very simple training and superior prediction accuracy. What is more, RBF networks can also lessen the influence of outlying values, what is in this particular case very useful because the measured data can contain noise and outlying values.

## II. RADIAL BASIS NEURAL NETWORKS

Radial basis function (RBF) neural networks are often used in various applications such as function approximation, time

series prediction and control. Generally two basic types of RBF networks are used: feed-forward [21]-[23] and recurrent [24], [25]. However, typical structure of radial basis neural networks is feed-forward and contains two layers. As is depicted in the Fig. 1, the hidden layer has radial basis function (RBF), whilst the linear transfer function is used in the output layer [4].

The radial basis function in the hidden layer is a function that normalizes radial distance between input vector  $\mathbf{u}$  and the vectors formed from the rows of weight matrix  $\mathbf{W}_1$ . The bias vector  $\mathbf{b}$  decides the range of influence of the particular RBF unit around its center defined in the matrix  $\mathbf{W}_1$ . General mathematical description of RBF networks is as follows [5]:

$$\mathbf{y} = S_2(\mathbf{b}_2 + \mathbf{W}_2 \mathbf{x}_1) \quad (1)$$

$$\mathbf{x}_1 = S_1(\|\mathbf{u} - \mathbf{W}_1 \mathbf{b}_1\|), \quad (2)$$

where  $\mathbf{y}$  is the output vector of the network,  $\mathbf{x}_1$  stands for the output vector of the hidden layer and  $S_i$  is transfer function of the  $i$ -th layer of the radial basis network.

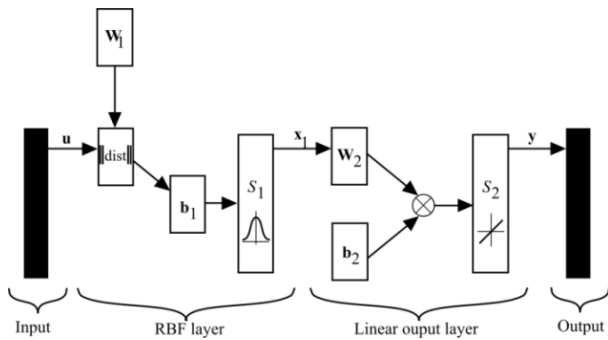


Fig. 1 Schema of radial basis function neural network

Radial basis networks are popular for their fast training and adaptation. However, these positives bring some disadvantages. The main drawback of RBF network is high memory requirement, because in the classic approach the number of neurons in the hidden layer is equal to the number of vectors of training data. Then, in the radial basis neural networks the weights  $\mathbf{W}_1$  and biases  $\mathbf{b}_1$  of the hidden layer are determined directly from the data. No training is involved. The weights  $\mathbf{W}_2$  and biases  $\mathbf{b}_2$  of the output layer are determined by supervised learning [6]. This methodology was adopted in the paper.

Though, there are more effective training methods such as parsimonious principle training [26], [27] that leads to less neurons in the hidden layer, but suffers overfitting; another approaches combine regularization with parsimonious principle to overcome the overfitting [28]-[30].

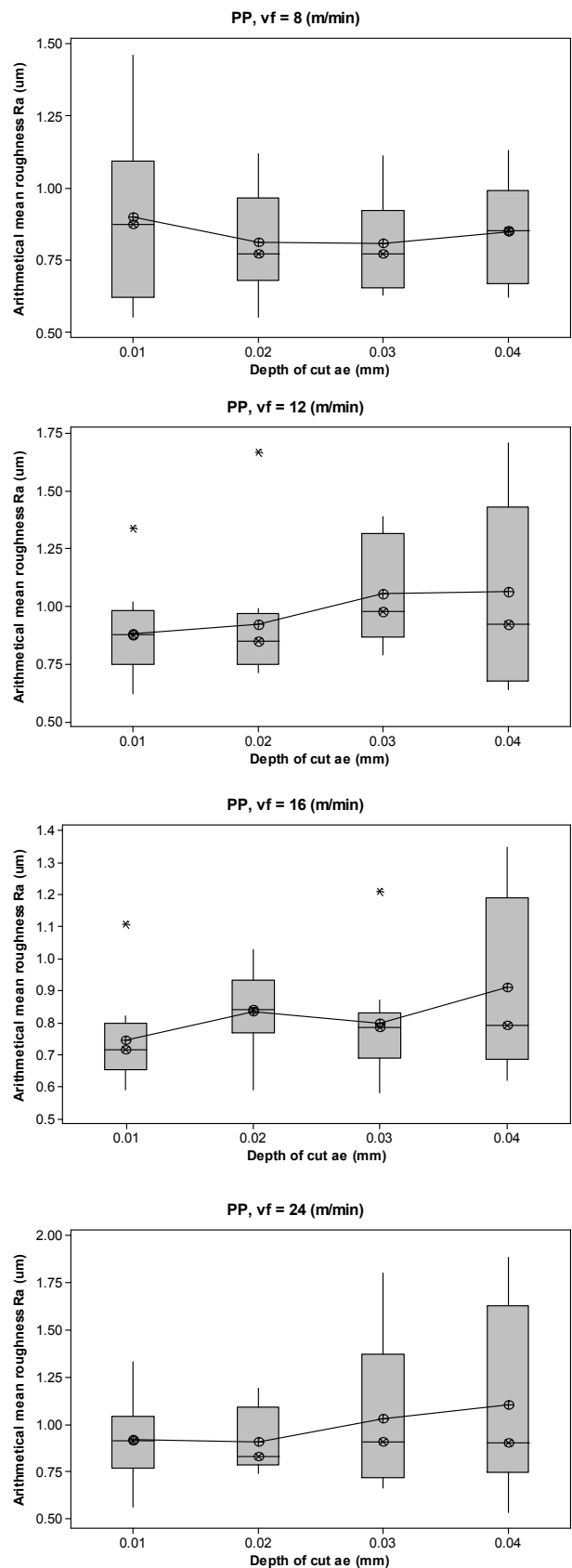


Fig. 2 The dependence of  $R_a$  on the depth of cut  $a_e$  for material PP for constant feed rate  $v_f$

## III. METHODOLOGY

For the experiment, polymer workpieces of block shape 50 x 50 x 20 mm were prepared from polypropylene (PP), polyamide 6 filled with 30% of glass fibres (PA6GF30), polytetrafluoroethylene (PTFE) and polycarbonate (PC) (details are in Table I). The Table I uses following nomenclature: MoE stands for modulus of elasticity (MPa), US for ultimate stress (MPa), MT for melting temperature ( $^{\circ}\text{C}$ ), and H for hardness (Shore).

Workpieces were attached to the surface grinding machine BRH 20.03F. Grinding wheel 99BA 46 J 9 V from sintered corundum with high porosity, that is recommended for polymer machining. Grinding was carried out with stroke back and forth, at specified cutting condition (Table II) without cooling. For the preparation of experimental specimens, the depth of cut and feed rate was changed while the grinding wheel revolution was constant.

Table I Physical and mechanical properties of polymer workpieces

|  | MoE<br>(MPa) | US<br>(MPa) | MT<br>( $^{\circ}\text{C}$ ) | H<br>(Shore) |
|--|--------------|-------------|------------------------------|--------------|
| PP- Polypropylene                                    | 1500         | 27          | 170                          | 70           |
| PA6GF30- Polyamide 6 filled with 30% of glass fibres | 7700         | 140         | 220                          | 86           |
| PTFE-Polytetrafluoroethylene                         | 500          | 30          | 320                          | 55           |
| PC - Polycarbonate                                   | 2200         | 65          | 140                          | 95           |

Prepared polymer specimens were measured using the stylus surface roughness tester Mitutoyo SJ-301 in the transverse direction to the feed rate vector. Measuring diamond tip radius was  $r_{\square} = 10$  mm and measurements were made according to ISO 4287. For the purpose of this study, measurements were multiple repeated at the same conditions.

Table II Conditions for the preparation of experimental specimens

|                                  |                                |
|----------------------------------|--------------------------------|
| Grinding wheel type              | 99BA 46 J 9 V                  |
| Grinding wheel size              | 250 x 20 x 76 (mm)             |
| Grinding wheel revolutions $n_w$ | 2550 ( $\text{min}^{-1}$ )     |
| Depth of cut $a_e$               | 0.01; 0.02; 0.03 and 0.04 (mm) |
| Feed rate $v_f$                  | 8, 12, 16, 24 (m/min)          |

## IV. SIMULATIONS AND RESULTS

The measured data were split into two parts. The first part was used for artificial neural network training, while the second group were processed and used as testing data for ANN verification.

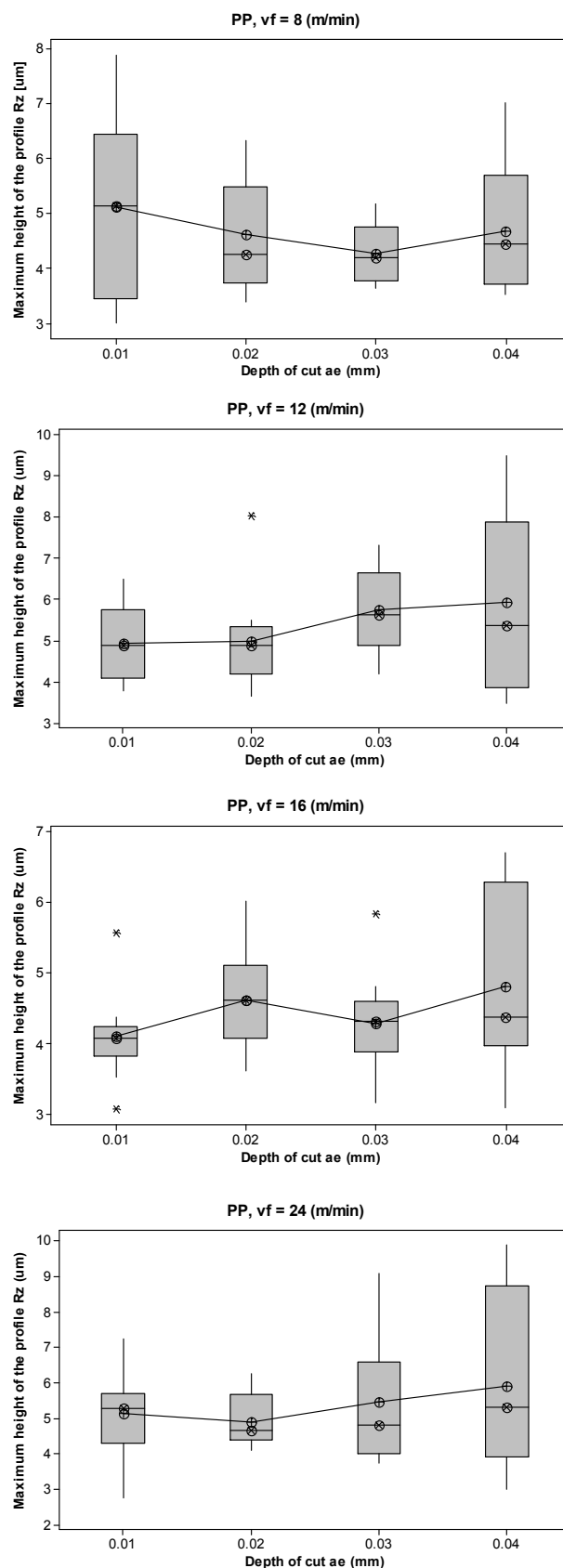


Fig. 3 The dependence of  $R_z$  on the depth of cut  $a_e$  for material PP for constant feed rate  $v_f$

All mathematical computations were done in MATLAB R2007b and MATLAB Neural Network Toolbox ver. 5.1. The RBF network was trained using build-in function (newrbe).

Table III Predicted values of  $R_a$  for PP

| $R_a$ ( $\mu\text{m}$ ) | $v_f$ (m/min) |        |        |        |
|-------------------------|---------------|--------|--------|--------|
| $a_e$ (mm)              | 8             | 12     | 16     | 24     |
| 0.01                    | 0.8990        | 0.8820 | 0.7450 | 0.9150 |
| 0.02                    | 0.8130        | 0.9249 | 0.8360 | 0.9071 |
| 0.03                    | 0.8060        | 1.0540 | 0.7981 | 1.0289 |
| 0.04                    | 0.8480        | 1.0640 | 0.9090 | 1.1020 |
| $R_z$ ( $\mu\text{m}$ ) | $v_f$ (m/min) |        |        |        |
| $a_e$ (mm)              | 8             | 12     | 16     | 24     |
| 0.01                    | 5.1112        | 4.9331 | 4.1012 | 5.1300 |
| 0.02                    | 4.6160        | 4.9768 | 4.6177 | 4.9015 |
| 0.03                    | 4.2691        | 5.7503 | 4.2865 | 5.4567 |
| 0.04                    | 4.6751        | 5.9270 | 4.8060 | 5.9053 |

There had to be created one ANN for each ground material. The predictor has two inputs (feed rate  $v_f$  and depth of cut  $a_e$ ) and two outputs describing surface roughness (arithmetical mean roughness  $R_a$  and maximum height of the profile  $R_z$ ). Predicted values for all materials are shown in tables III – VI.

After that, the predictors were subjected to verification using the second part of data. The verification data were statistically evaluated. Then, the mean values were computed for each combination of input parameters. These mean values (Fig. 2-17) were compared to the predicted data.

As can be seen from figures, the predictors provide excellent predictions of desired output parameters for all tested polymers.

Table IV Predicted results for PA6GF30

| $R_a$ ( $\mu\text{m}$ ) | $v_f$ (m/min) |        |        |        |
|-------------------------|---------------|--------|--------|--------|
| $a_e$ (mm)              | 8             | 12     | 16     | 24     |
| 0.01                    | 0.5889        | 0.6250 | 0.4490 | 0.5360 |
| 0.02                    | 0.5320        | 0.5800 | 0.4850 | 0.5740 |
| 0.03                    | 0.5640        | 0.5150 | 0.7290 | 0.5550 |
| 0.04                    | 0.5320        | 0.4990 | 0.6250 | 0.5340 |
| $R_z$ ( $\mu\text{m}$ ) | $v_f$ (m/min) |        |        |        |
| $a_e$ (mm)              | 8             | 12     | 16     | 24     |
| 0.01                    | 3.8125        | 4.0379 | 2.9893 | 3.3909 |
| 0.02                    | 3.3337        | 3.6366 | 3.0759 | 3.6727 |
| 0.03                    | 3.3390        | 3.3112 | 4.8340 | 3.4910 |
| 0.04                    | 3.2867        | 3.0759 | 3.8360 | 3.3026 |

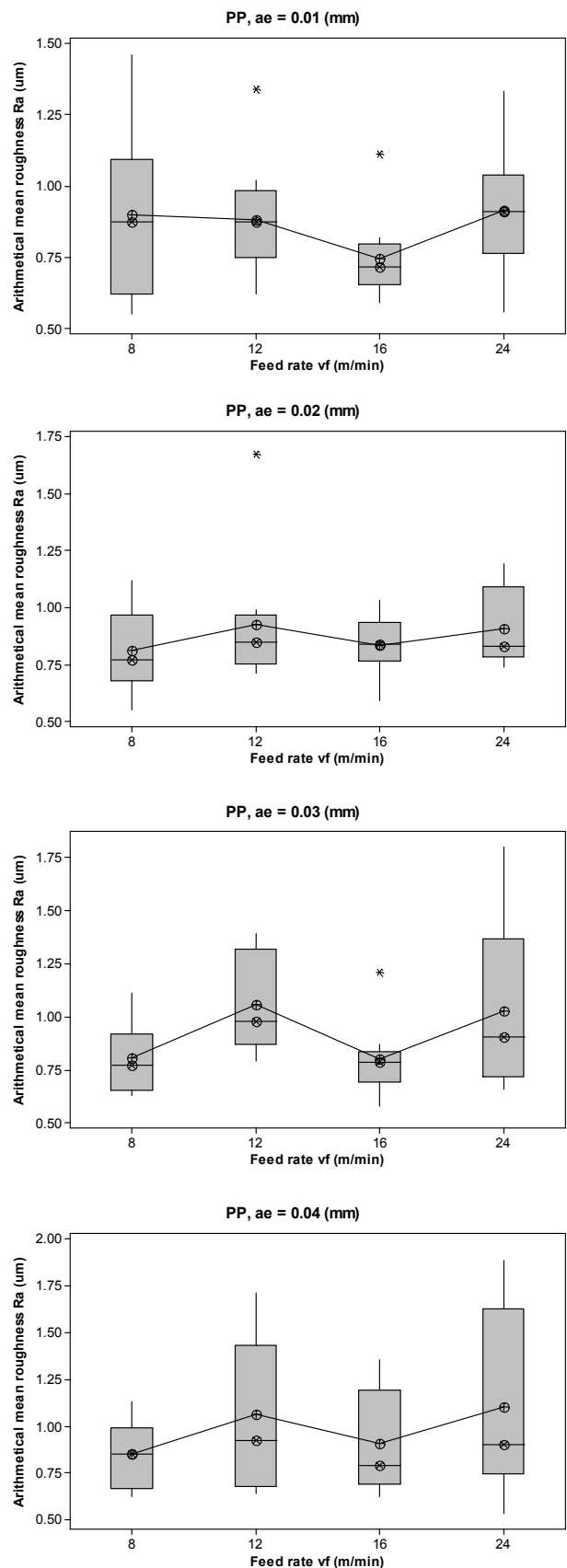


Fig. 4 The dependence of  $R_a$  on the feed rate  $v_f$  for material PP for constant depth of cut  $a_e$

Table V Predicted results for PTFE

| $R_a$ ( $\mu\text{m}$ ) | $v_f$ (m/min) |        |        |        |
|-------------------------|---------------|--------|--------|--------|
| $a_e$ (mm)              | 8             | 12     | 16     | 24     |
| 0.01                    | 0.3920        | 0.6040 | 0.5090 | 0.7180 |
| 0.02                    | 0.5450        | 0.6290 | 0.5201 | 0.5280 |
| 0.03                    | 0.5350        | 0.7810 | 0.6121 | 0.6500 |
| 0.04                    | 0.6120        | 0.5640 | 0.6621 | 0.6500 |
| $R_z$ ( $\mu\text{m}$ ) | $v_f$ (m/min) |        |        |        |
| $a_e$ (mm)              | 8             | 12     | 16     | 24     |
| 0.01                    | 2.2219        | 3.4180 | 2.7301 | 3.8990 |
| 0.02                    | 3.0070        | 3.3401 | 2.8902 | 2.8369 |
| 0.03                    | 2.9970        | 4.0399 | 3.3591 | 3.4941 |
| 0.04                    | 3.4260        | 3.0200 | 3.5012 | 3.4659 |

Table VI Predicted results for PC

| $R_a$ ( $\mu\text{m}$ ) | $v_f$ (m/min) |        |        |        |
|-------------------------|---------------|--------|--------|--------|
| $a_e$ (mm)              | 8             | 12     | 16     | 24     |
| 0.01                    | 0.6751        | 0.8590 | 0.5690 | 0.6660 |
| 0.02                    | 0.6361        | 0.7680 | 0.7000 | 0.6860 |
| 0.03                    | 0.7270        | 0.6520 | 0.7160 | 0.7470 |
| 0.04                    | 0.9811        | 0.7990 | 0.8850 | 0.6820 |
| $R_z$ ( $\mu\text{m}$ ) | $v_f$ (m/min) |        |        |        |
| $a_e$ (mm)              | 8             | 12     | 16     | 24     |
| 0.01                    | 3.5323        | 4.3191 | 3.1059 | 3.6260 |
| 0.02                    | 3.1602        | 4.0151 | 3.6220 | 3.6770 |
| 0.03                    | 3.6331        | 3.5331 | 3.7849 | 3.8320 |
| 0.04                    | 4.7112        | 3.8961 | 4.7359 | 3.5511 |

V. MEASUREMENT EVALUATION

To evaluate the grinding process, box plots were chosen to graphically characterize the shape of the distribution, the mean and variability. In the box plots (Fig. 2 to 17) can be seen the values of roughness parameters  $R_a$  and  $R_z$ . Where the middle line in the box with the x symbol represents the median, and the + symbol represents the mean. Boundaries of boxes represent the first and third quartile, which is 50% of all measured values. The area between first and third quartile indicate the interquartile range (IQR). Extreme values ( $1.5 \times \text{IQR}$ ) are the limit line, which is 25% of the values of the lowest and highest values. Points that are located at a distance greater than  $1.5 \times \text{IQR}$  from the median are shown as asterisk. These points represent the possible devious measurement.

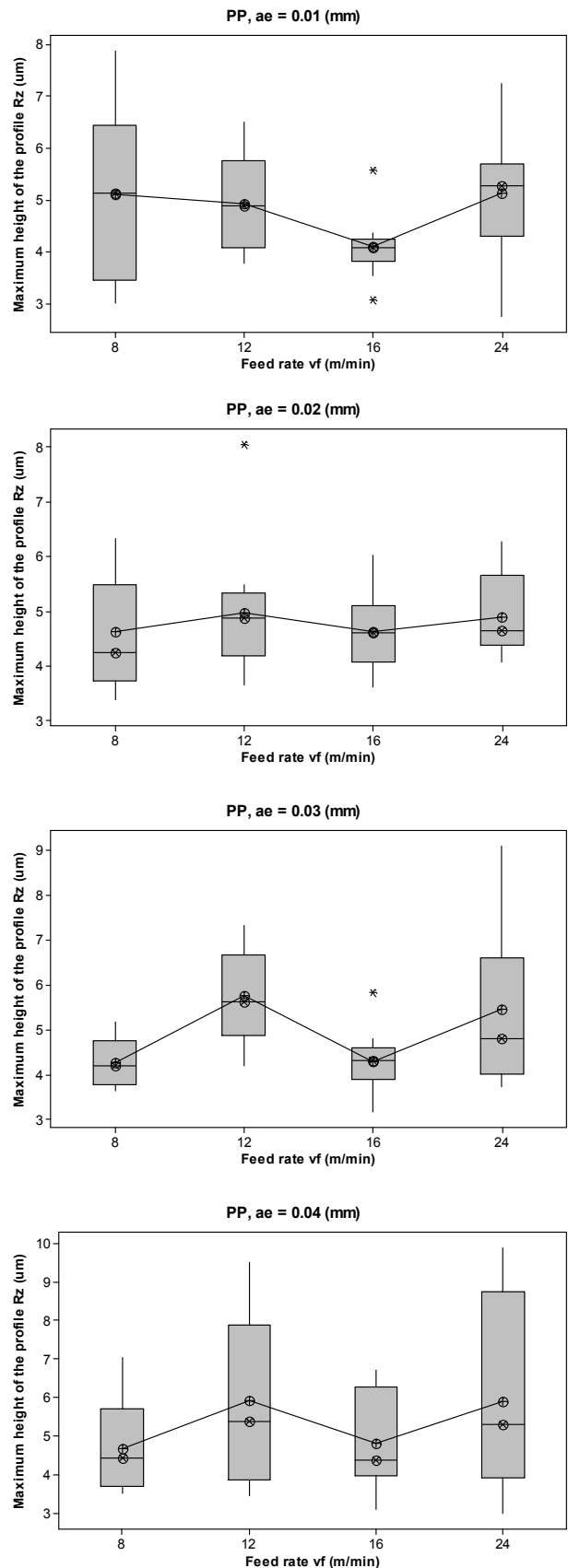


Fig. 5 The dependence of  $R_z$  on the feed rate  $v_f$  for material PP for constant depth of cut  $a_e$

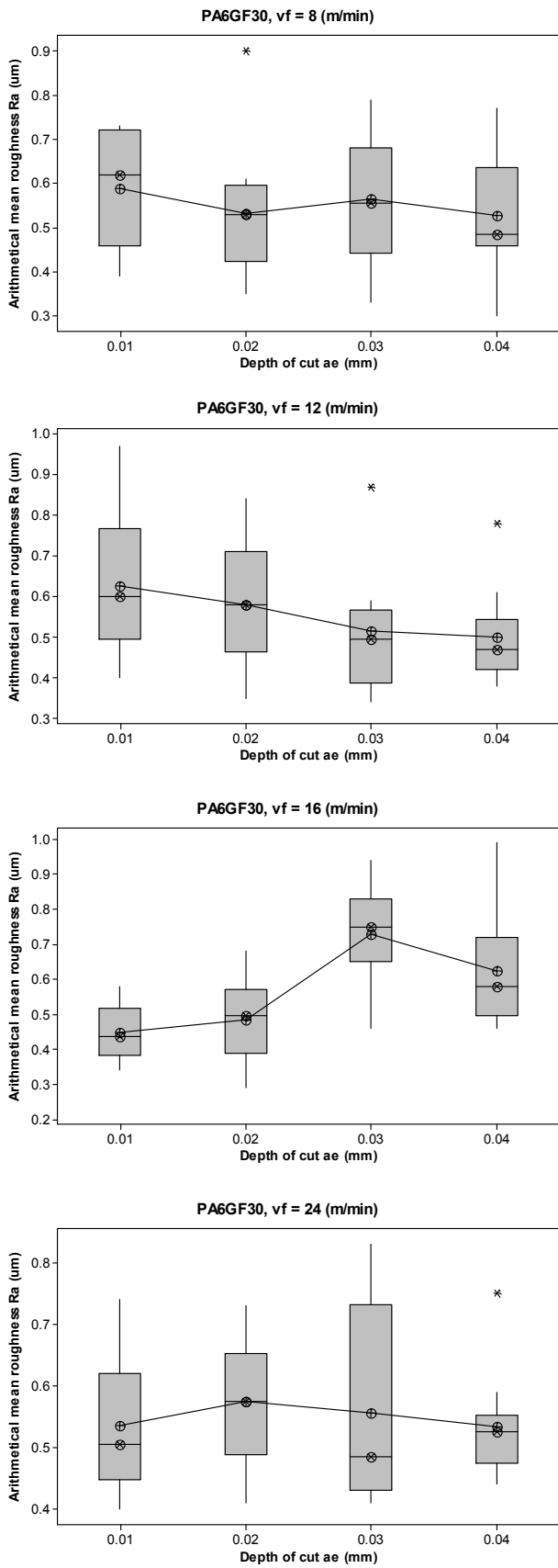


Fig. 6 The dependence of  $R_a$  on the depth of cut  $a_e$  for material PA6GF30 for constant feed rate  $v_f$

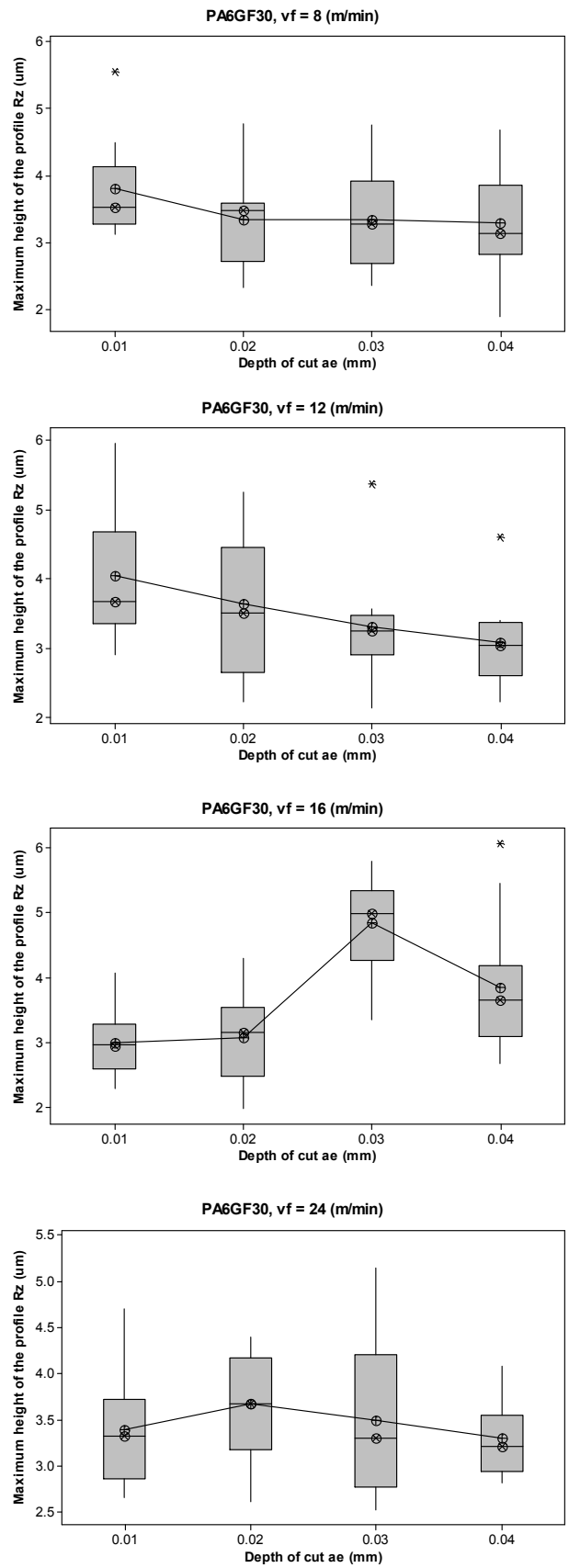


Fig. 7 The dependence of  $R_z$  on the depth of cut  $a_e$  for material PA6GF30 for constant feed rate  $v_f$

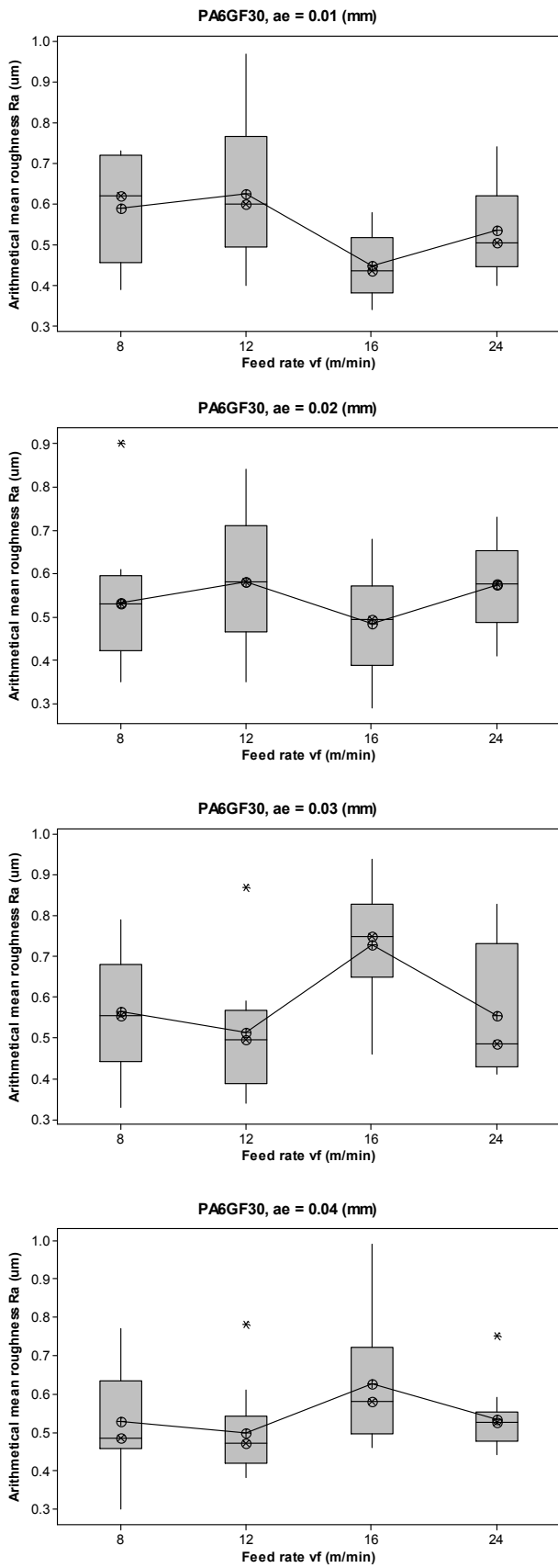


Fig. 8 The dependence of  $R_a$  on the feed rate  $v_f$  for material PA6GF30 for constant depth of cut  $a_e$

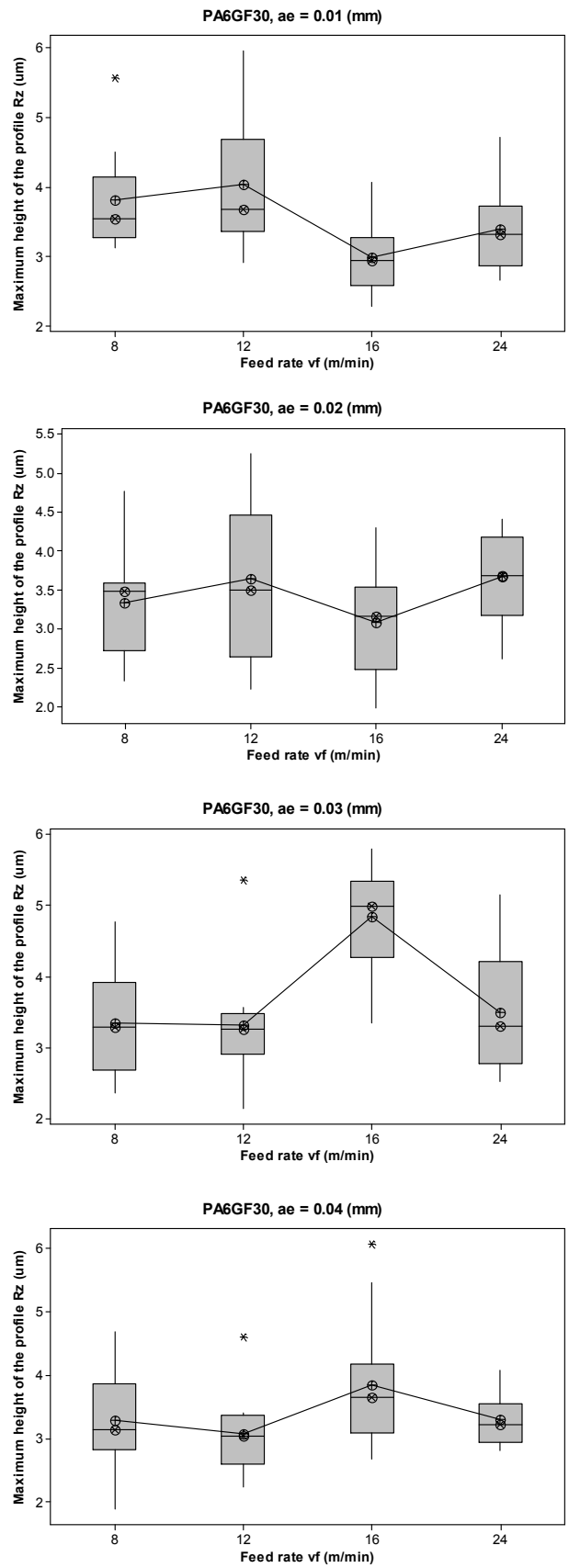


Fig. 9 The dependence of  $R_z$  on the feed rate  $v_f$  for material PA6GF30 for constant depth of cut  $a_e$

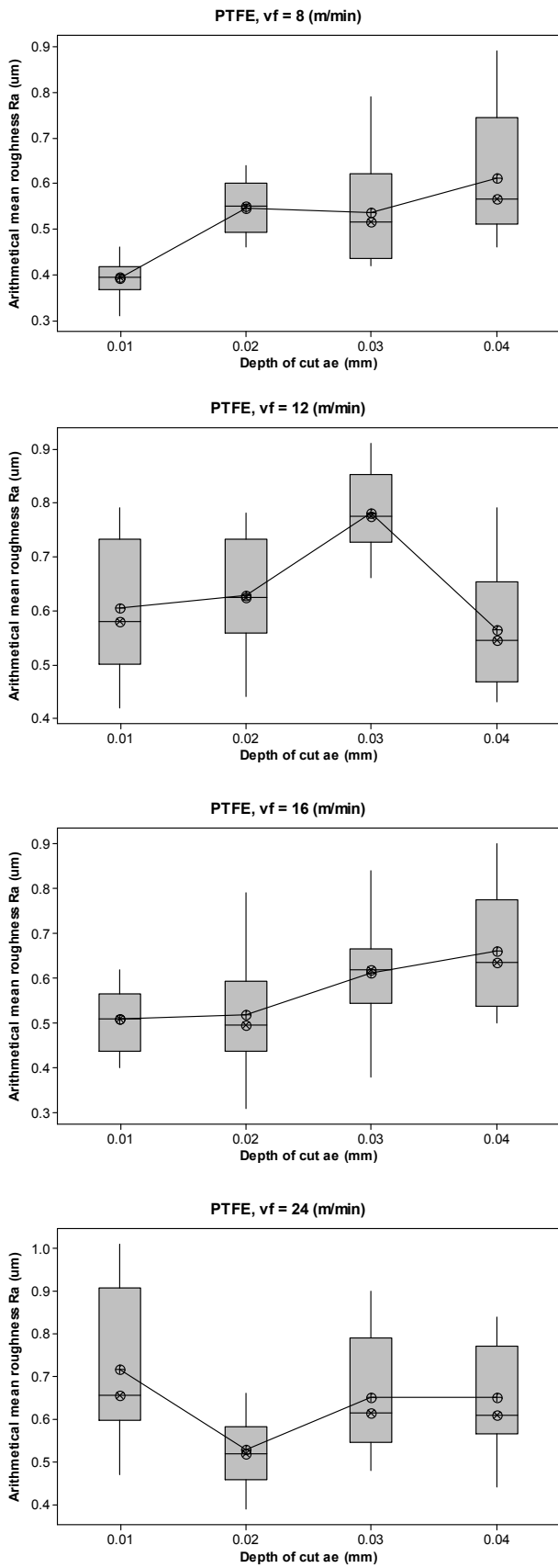


Fig. 10 The dependence of  $R_a$  on the depth of cut  $a_e$  for material PTFE for constant feed rate  $v_f$

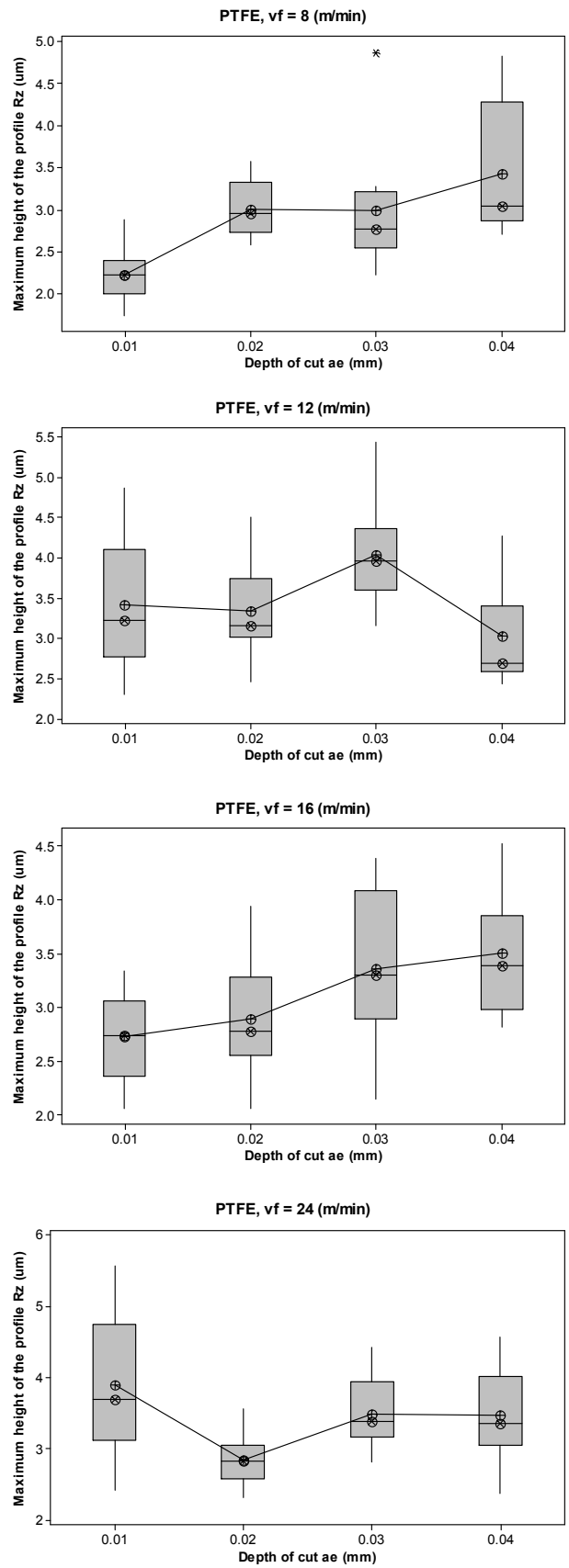


Fig. 11 The dependence of  $R_z$  on the depth of cut  $a_e$  for material PTFE for constant feed rate  $v_f$

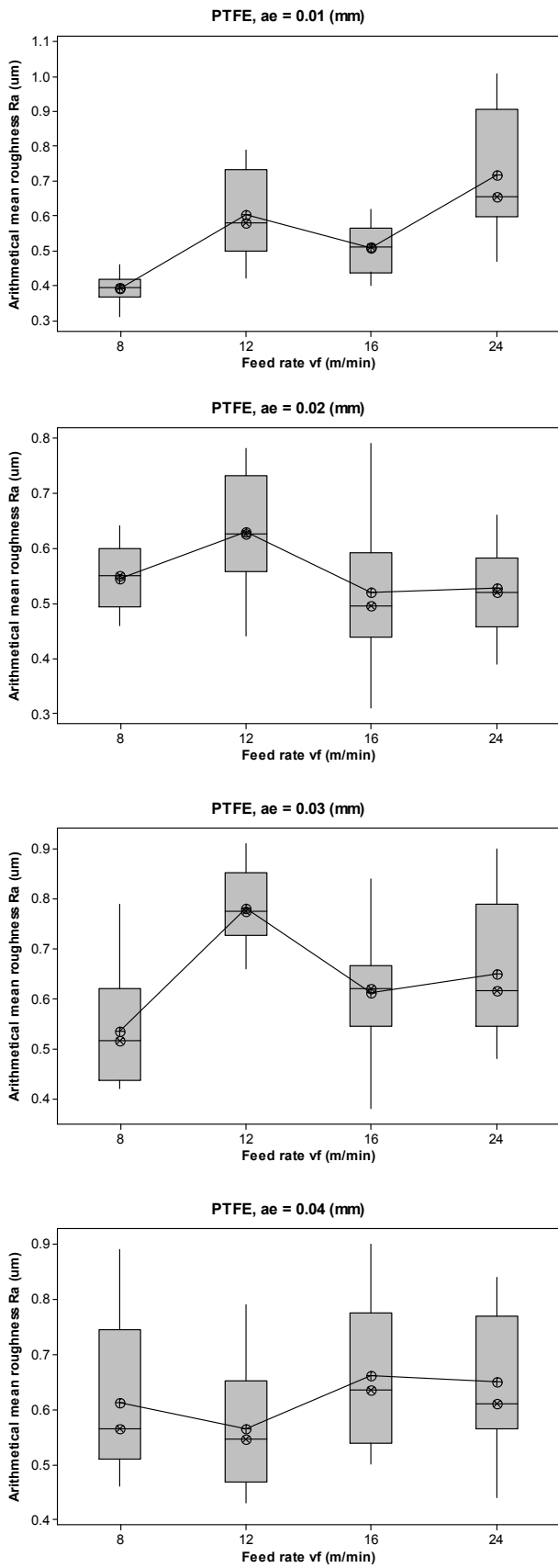


Fig. 12 The dependence of  $R_a$  on the feed rate  $v_f$  for material PTFE for constant depth of cut  $a_e$

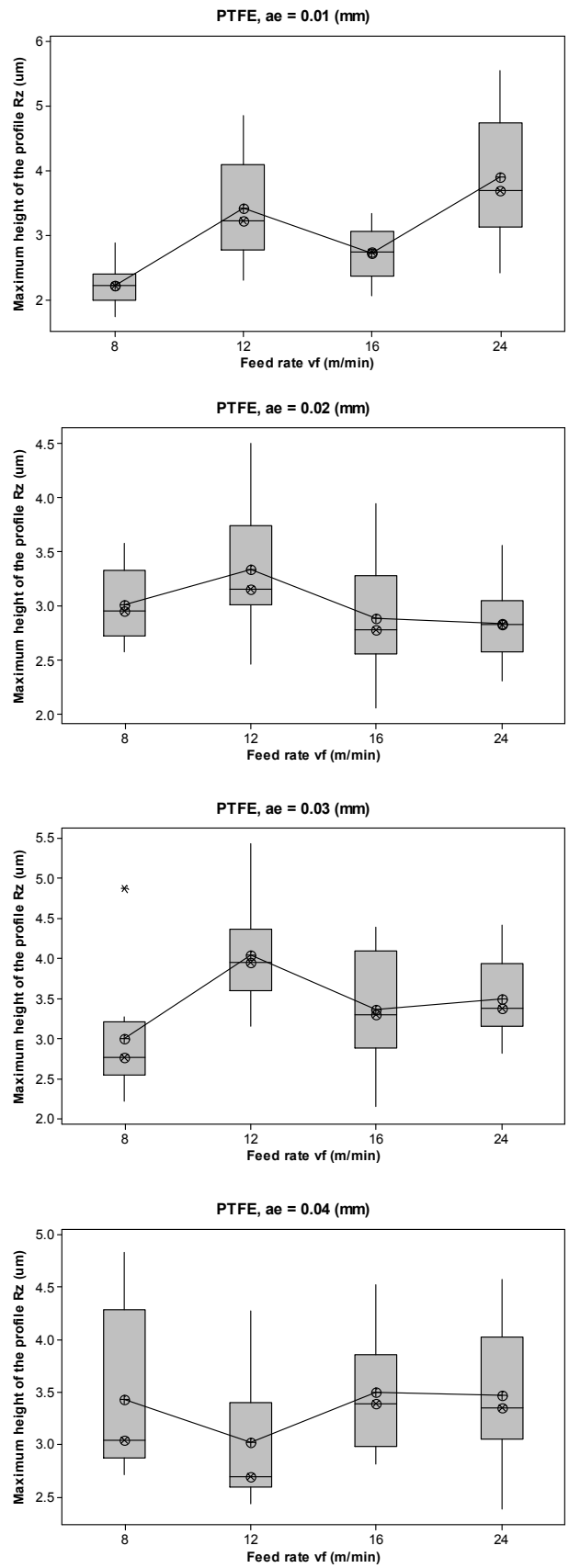


Fig. 13 The dependence of  $R_z$  on the feed rate  $v_f$  for material PTFE for constant depth of cut  $a_e$

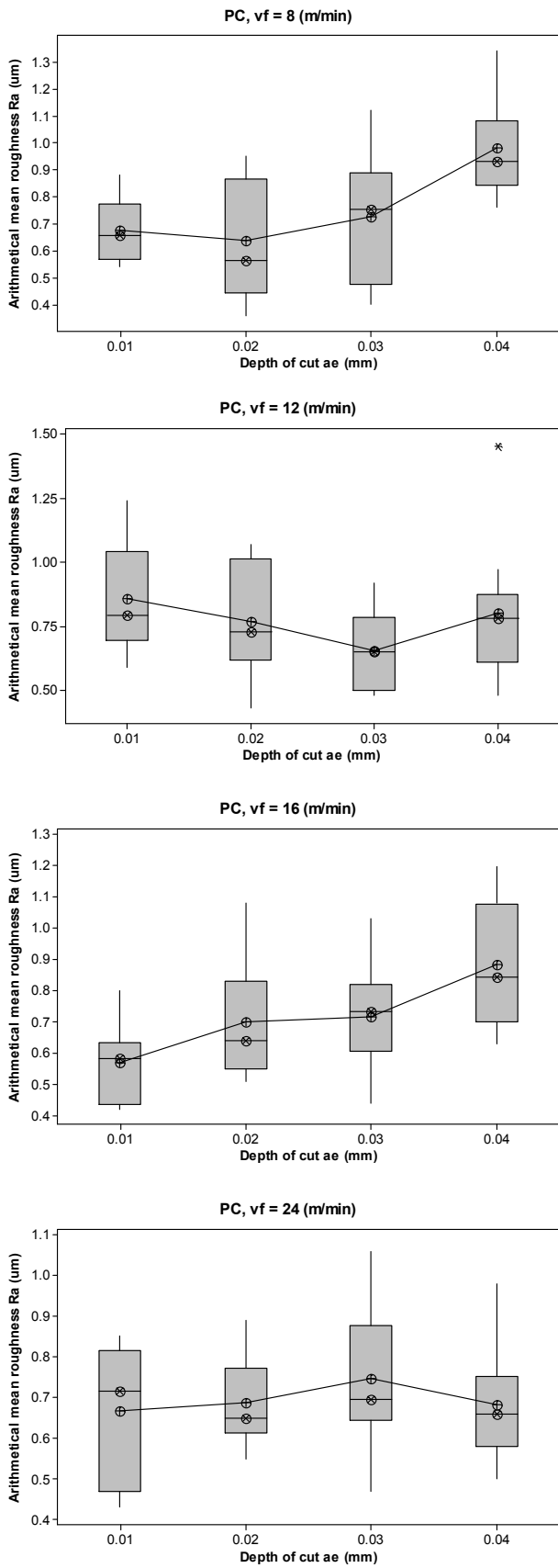


Fig. 14 The dependence of  $R_a$  on the depth of cut  $a_e$  for material PC for constant feed rate  $v_f$

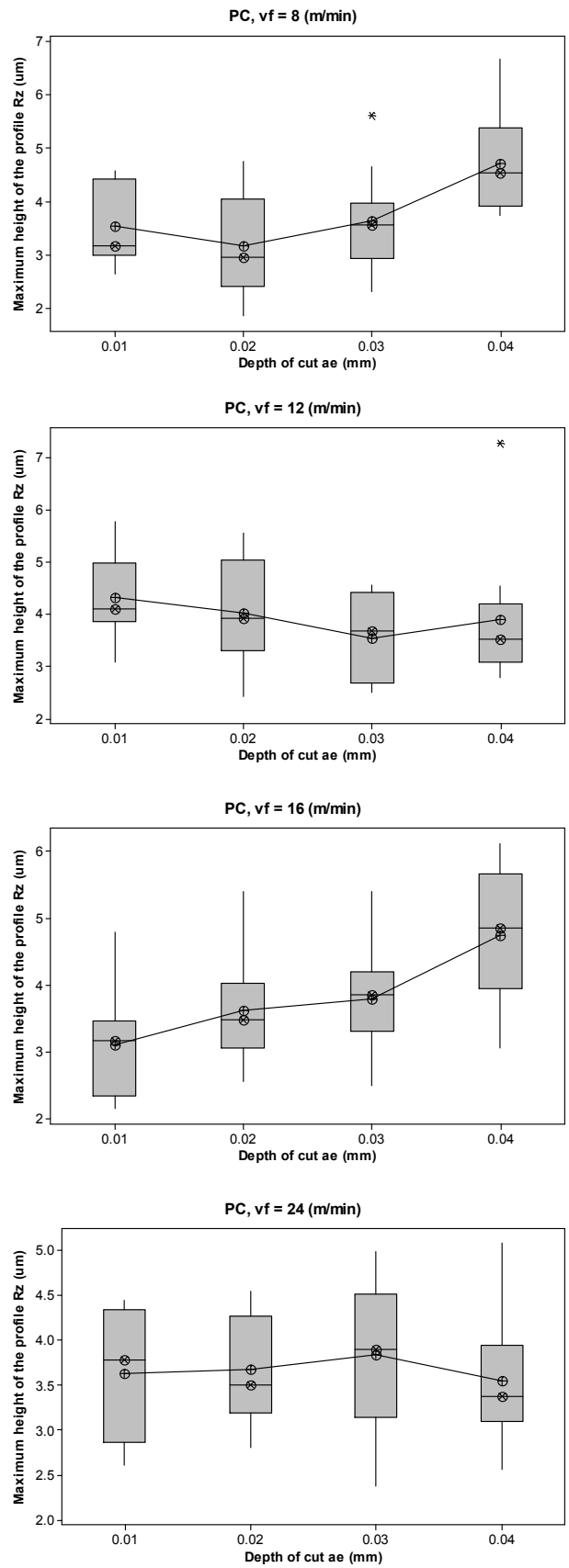


Fig. 15 The dependence of  $R_z$  on the depth of cut  $a_e$  for material PC for constant feed rate  $v_f$

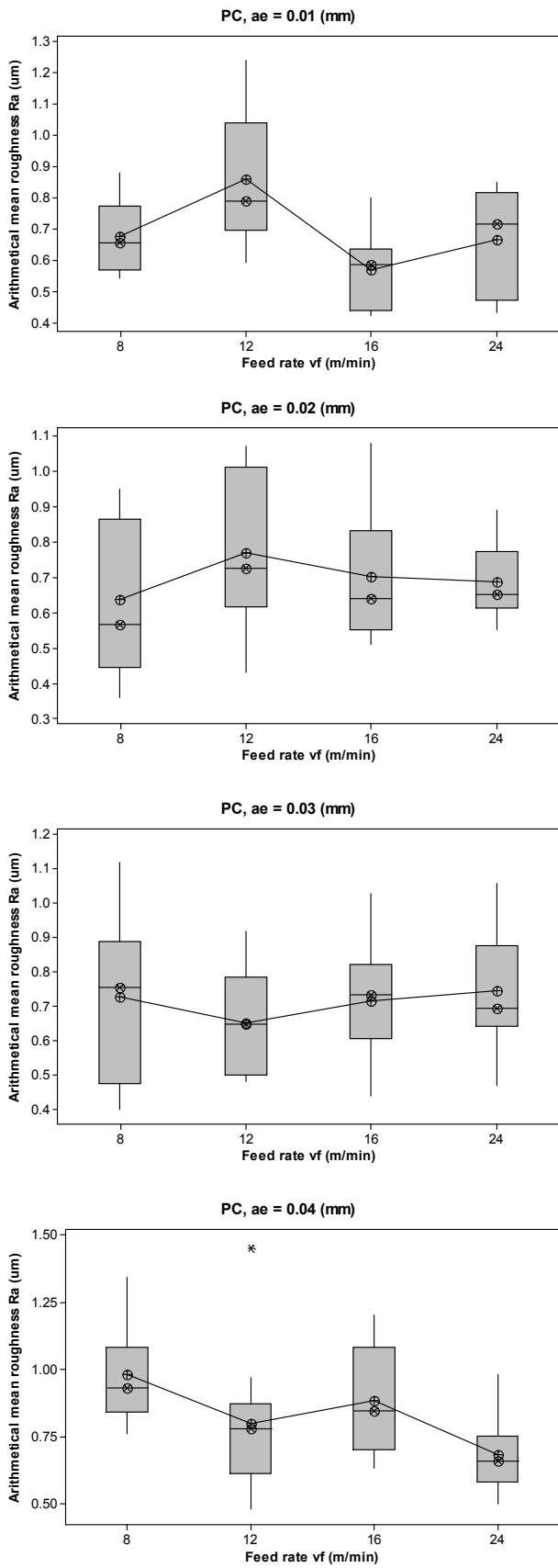


Fig. 16 The dependence of  $R_a$  on the feed rate  $v_f$  for material PC for constant depth of cut  $a_e$

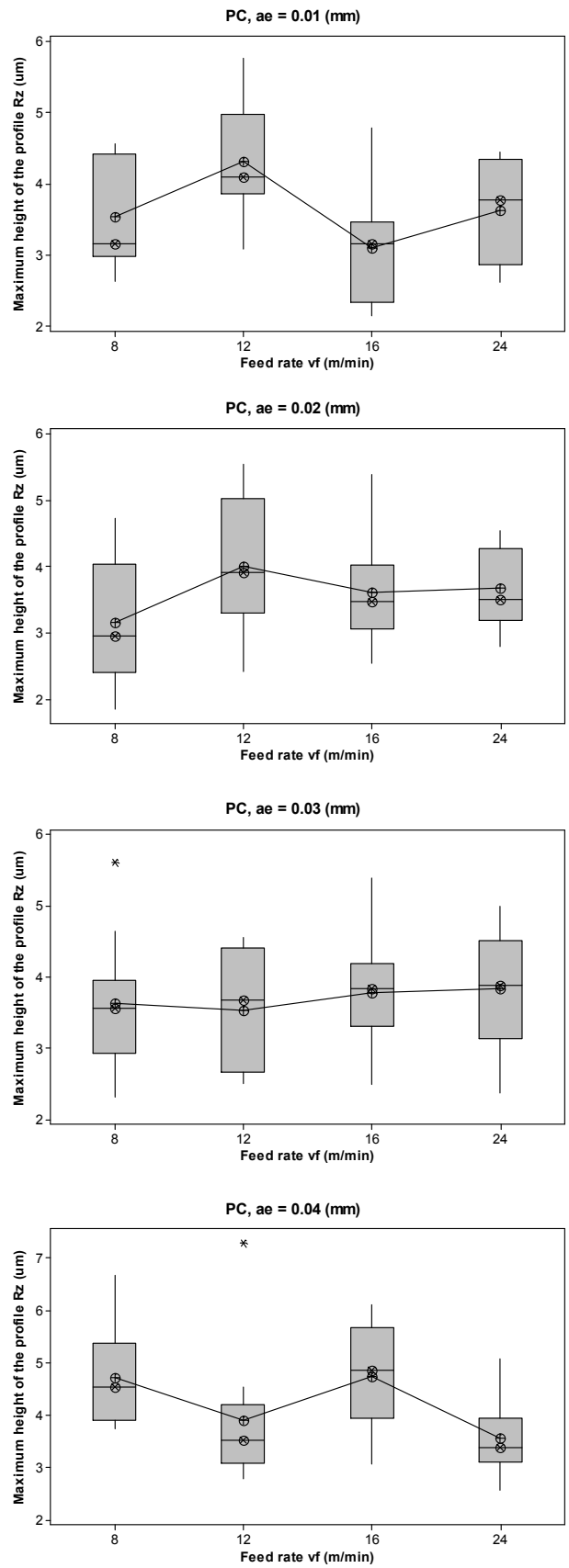


Fig. 17 The dependence of  $R_z$  on the feed rate  $v_f$  for material PC for constant depth of cut  $a_e$

Based on graphical evaluation was found that the material PP (Fig. 2-5) has the mean roughness parameter  $R_a$  values in the range from 0.9 to 1.1  $\mu\text{m}$ . The actual measurement was influenced by grinding grains, remained bonded on the surface, leading to difficult quantification of roughness parameters. Moreover while grinding; melted chips are adhered on the grinding wheel as well as on the surface material, which has a negative effect on surface roughness. Generally, the material PP is difficult to grind. The material PA6GF30 falls into the group medium-grindable material. The values of roughness  $R_a$  are ranging from 0.4 to 0.7  $\mu\text{m}$  (Fig. 6 – 9). It is possible to observe that the narrow range of measured values of mean roughness  $R_a$  affects glass reinforcement of the material.

PTFE material (Fig. 10- 13) also exhibits low roughness values for all variables (feed rate, depth of cut). The mean values of roughness parameter  $R_a$  are ranging from 0.4 to 0.8  $\mu\text{m}$ . It is possible to say that to the increasing depth of cut roughness parameter increases approximately in direct proportion. An interesting feature of this material is greater heat generation during the grinding, compared to the other materials, resulting in deterioration of ground surface.

The PC material belongs to a group of material very well to grind. The mean values of roughness parameter  $R_a$  (Fig. 14 - 17) are ranging from 0.6 to 1.0  $\mu\text{m}$ . Similarly to PTFE material, increasing depth of cut has adverse effect on the surface quality.

From box plots (Fig. 2 -17) is not entirely clear, but the assembled statistical model [11] determined that feed rate  $v_f$  does not affect roughness parameter  $R_a$ . An important variable in the grinding process not only for metal materials but also for plastics, as shown in this study, is the depth of cut  $a_e$ , to the extent that increasing depth of cut deteriorates the final surface quality.

## VI. CONCLUSION

This paper presented application of artificial neural networks to modeling of industrial process. The obtained predictions were even surprisingly good. It is probably caused by the nature of the real measured data. Because the data were very noised and obtained lot of outlying values, it was necessary to use radial basis neural network that in this case produces approximately mean of the training data.

## REFERENCES

- [1] C. Dang, T. Ji and X. Jiang, "Research on the Stability Problem of Hydroelectric Station Penstock under External Pressure Based on Neural Network," *WSEAS TRANSACTIONS on APPLIED and THEORETICAL MECHANICS*, vol.5, no.1, pp. 1-10, January 2010.
- [2] D. Samek and L. Sykorova, "Feed-forward neural network model verification and evaluation," in *Annals of DAAAM for 2010 and Proc. of 21st Int. DAAAM Symp.: Intelligent Manufacturing & Automation: Focus on Interdisciplinary Solutions*. Zadar, 2010, pp. 583-584.
- [3] L. Sykorova, "Cutting depth determination within CO<sub>2</sub> laser micromachining," in *Annals of DAAAM for 2010 and Proceedings of the 17th International DAAAM Symposium*. Vienna, 2006, pp.405-406.
- [4] J. A. K. Suykens, J. P. L. Vandewalle and B. L. R. De Moor, *Artificial Neural Networks for Modeling and Control of Non-Linear Systems*, Dordrecht: Kluwer AP, 1996.
- [5] O. Nelles, *Nonlinear system identification*, Berlin: Springer, 2001.
- [6] B. Yegnanarayana, *Artificial Neural Networks*, New Delhi: Prentice-Hall of India, 1999.
- [7] M. Alauddin, I. A. Choudhury, M. A. El Baradie and M. S. J. Hashmi, "Plastics and their machining: a review," *Journal of Materials Processing Technology*, vol. 54, no. 1, pp. 40-46, October 1995.
- [8] I. Lukovics and K. Kocman, "Thermodynamic Effects when Precision Grinding," *Manuf. Tech.*, vol. 10, no. 4, pp. 117-121, Dec. 2005.
- [9] N. D. Stanescu, "Chaos in Grinding Process," in *WSEAS TRANSACTIONS on APPLIED and THEORETICAL MECHANICS*, vol. 4, no. 4, pp. 195-204, October 2009.
- [10] J. Madl, J. Jersak and F. Holesovsky, *Quality of machined surfaces (Jakost obrabenych povrchu)*. Usti nad Labem: UJEP, 2003.
- [11] O. Bilek, I. Lukovics and L. Rokyta, "Manufacturing of Thermoplastics and Chip Formation," *Chem. Listy*, vol. 105, pp.317-319, Apr. 2011.
- [12] I. Bogdanov, R. Mirsu and V. Tiponut, "MATLAB model for spiking neural networks," in *Proceedings of the 13th WSEAS International Conference*, Rhodes Isl., 2009, pp. 533-537.
- [13] S. Erkaya and S. Yildirim, "Evaluation of noise characteristics for a cooling system using Neural Network," in *11th WSEAS International Conference*, Venice, 2011, pp. 39-45.
- [14] A. R. Fazeli Nahrekhalaji, "Statistical modeling of root geometrical dimensions of gas turbine blade in creep feed grinding process," in *Proc. of the 10th WSEAS Int. Conference on Robotics, Control and Manufacturing Technology, ROCOM '10*, Hangzhou, 2010, pp. 79-84.
- [15] A. Epureanu, V. Teodor and N. Oancea, "Topological modelling of the part geometry in manufacturing," in *Proc. of the 11th WSEAS Int. Conference on Mathematical Methods, Computational Techniques and Intelligent Systems, MAMECTIS '09, Proc. 8th WSEAS NOLASC '09, Proc. 5th WSEAS CONTROL '09*, Lalaguna, 2009, pp. 75-80.
- [16] M. Neslusan, et. al., *Experimental Methods in Chip Working*. Zilina: Zilinska univerzita v Ziline, 2007.
- [17] P. R. Aguiar, C. E. D. Cruz, W. C. F. Paula, E. C. Bianchi, R. Thomayella and F. R. L. Dotto, "Neural network approach for surface roughness prediction in surface grinding," in *Proceedings of the IASTED International Conference on Artificial Intelligence and Applications*, Innsbruck, 2007, pp. 96-101.
- [18] J. Madl, "Design for Machining," *Manufacturing Technology*, vol. 9, no. 4, pp 81-86, December 2009.
- [19] J. Kundrak, W. Zebala and V. Bana, "Examination of Cutting Zone Deformation Occurring," *Manuf. Tech.*, vol. 3, no. 1, pp 3-7, 2003.
- [20] I. Lukovics and L. Sykorova "Det. of grinding wheels cutting property for high performance grinding," in *Tools 99*, Zlin, 1999, pp. 1-7.
- [21] X. Yao, X. Zhang, R. Zhang, M. Liu, Z. Hu and B. Fan, "Prediction of enthalpy of alkanes by the use of radial basis function neural networks," *Computers & Chemistry*, vol. 25, no. 5, pp. 475-482, September 2001.
- [22] D. Casasent and X. Chen, "Radial basis function neural networks for nonlinear Fisher discrimination and Neyman-Pearson classification," *Neural Networks*, vol. 16, no. 5-6, pp. 529-535, June-July 2003.
- [23] R. Kumar, R. Ganguli and S. N. Omkar, "Rotorcraft parameter estimation using radial basis function neural network," *Applied Mathematics and Computation*, vol. 216, no. 2, pp. 584-597, Mar 2010.
- [24] R. Zemouri, D. Racoceanu and N. Zerhouni, "Recurrent radial basis function network for time-series prediction," *Engineering Applications of Artificial Intelligence*, vol. 16, no. 5-6, pp. 453-463, Aug-Sep. 2003.
- [25] Ch. Venkateswarlu and K. V. Rao, "Dynamic recurrent radial basis function network model predictive control of unstable nonlinear processes," *Chem. Eng. Sc.*, vol. 60, no. 23, pp. 6718-6732, Dec 2005.
- [26] S. Chen, C. F. N. Cowan and P. M. Grant, "Orthogonal least squares algorithm for radial basis function networks," *IEEE Transactions on Neural Networks*, vol. 2, no. 2, pp. 302-309, March 1991.
- [27] T. Kavli, "ASMOD an algorithm for adaptive spline modeling of observation data," *Int. J. of Control*, vol. 58, no. 4, pp. 947-968, 1993.
- [28] A. R. Barron and X. Xiao, "Discussion of multivariate adaptive regression splines," *Annals. of Statistics*, vol. 19, no. 1, pp. 67-82, March 1991.
- [29] S. Chen, E. S. Chng and K. Alkadhimi, "Regularized orthogonal least squares algorithm for constructing radial basis function networks," *International Journal of Control*, vol. 64, no. 5, pp. 829-937. Jul 1996.
- [30] Z. Wang and T. Zhu, "An efficient learning algorithm for improving generalization performance of radial basis function neural networks," *Neural Networks*, vol. 13, no. 4-5, pp. 545-553, June 2000.